Available online at www.sciencedirect.com
ScienceDirect
Journal of Molecular Catalysis A: Chemical 280 (2008) 35–42
JOURNAL OF MOLECULAR CATALYSIS A: CHEMICAL
www.elsevier.com/locate/molcata

Impact of temperature ramping rate during calcination on characteristics of nano-ZrO_2 and its catalytic activity for isosynthesis

Watcharapong Khaodee [a], Bunjerd Jongsomjit [a], Piyasan Praserthdam [a], Shigeo Goto [b], Suttichai Assabumrungrat [a,*]

[a] *Center of Excellence in Catalysis and Catalytic Reaction Engineering, Department of Chemical Engineering, Faculty of Engineering, Chulalongkorn University, Bangkok 10330, Thailand*
[b] *Department of Chemical Engineering, Nagoya University, Chikusa, Nagoya 464-8603, Japan*

Received 1 February 2007; received in revised form 16 October 2007; accepted 17 October 2007
Available online 23 October 2007

Abstract

This paper studied the effect of temperature ramping rate during calcination on characteristics of nanoscale zirconia and its catalytic performance for isosynthesis. The physical properties, i.e. BET surface area, cumulative pore volume, cumulative pore diameter and the phase composition in zirconia, acid-base properties and surface properties such as Zr^{3+} quantity, were characterized. Increase in the temperature ramping rate of calcination resulted in a higher composition of the tetragonal phase, but it showed insignificant influence on the other physical properties. Considering the catalytic activity, the acid sites did not affect the activity, but the basic sites depended on the fraction of the tetragonal phase in zirconia which was related to the selectivity to isobutene. The intensity of Zr^{3+} on the surface varied with the change in the heating rate of calcination. Both the tetragonal phase composition in zirconia and the quantity of Zr^{3+} were the key factors affecting the selectivity to isobutene in hydrocarbons. Moreover, the maximum value of the product selectivity to isobutene on the ZrO_2 (5.0) catalyst was attained at the highest concentration of Zr^{3+}.

Keywords: Isosynthesis; Tetragonal phase; ZrO_2; Zr^{3+}; Isobutene

1. Introduction

At present, the octane enhancer demand is continuously increasing with the increased fuel consumption. Isobutene is an important raw material for the production of important octane enhancers such as methyl *tert*-butyl ether (MTBE) and ethyl *tert*-butyl ether (ETBE). Typically, isobutene is extracted from the C_4 stream in petroleum refining process; however, the supply of isobutene from the petroleum products is possibly inadequate in the near future. It is expected that an alternative source for the production of isobutene needs to be explored. It is evident that one of the promising sources for isobutene synthesis can be provided by syngas derived from a renewable resource such as biomass. This route is attractive due to the following reasons (i) the chosen resource of isobutene production is renewable, then being more green than the conventional petroleum sources, which are about to face shortage in the near future, (ii) carbon dioxide, a by-product of fermentation process, is substantially consumed to produce syngas, thus reducing the CO_2 emission to the atmosphere and (iii) the ratio of carbon monoxide to hydrogen of 1:1 for the syngas from fermentation of biomass is suitable for the reaction of isobutene synthesis.

As is well known, isosynthesis is the catalytic reaction that converts syngas to branched chain hydrocarbons, especially isobutane and isobutene. The early work [1] showed that suitable catalysts for the isosynthesis reaction are hardly reducible oxides such as zirconia rather than other reduced transition metals. It has been reported that zirconia is the most selective catalyst for isosynthesis [2–6]. The effect of characteristics of catalysts on their catalytic performance was investigated by some researchers. For instance, the characteristic and catalytic performance of the nanoscale zirconias prepared by various methods

* Corresponding author. Tel.: +662 218 6868; fax: +662 218 6877.
E-mail address: Suttichai.A@chula.ac.th (S. Assabumrungrat).

1381-1169/$ – see front matter © 2007 Elsevier B.V. All rights reserved.
doi:10.1016/j.molcata.2007.10.020

such as the precipitation method, the supercritical fluid drying method and the freeze-drying method for isosynthesis were studied by Su et al. [4]. They found that the different preparation methods affected catalytic performance, and better product selectivity of isobutene resulted from higher ratios of base to acid sites on the catalyst surface. As reported by Maruya et al. [6], the crystal phases such as monoclinic phase in zirconia influenced catalytic performance. Moreover, the acidity and basicity could play an important role on the catalytic performance because of bifuntionality of zirconia [4,7–9]. In addition, effects of these factors such as crystallite size, the phase composition and acid-base sites of zirconia on catalytic performance were also studied in our previous paper [10]. However, the studies of surface properties of catalysts such as acid-base sites related with the crystal phase of zirconia and the quantity of Zr^{3+} on the surface were not investigated. From the study of Zr^{3+} [11], it was found that Zr^{3+} ion was related to the selectivity to isobutene in the reaction on zirconia.

In this work, the effect of temperature ramping rate during calcination on characteristics and catalytic performance for isosynthesis of zirconia catalysts was investigated. The synthesized nanoscale zirconia catalysts were prepared using the precipitation method. Various physical characteristics of zirconia catalysts such as the phase composition in zirconia, acid-base properties and surface properties including quantity of Zr^{3+} on the catalyst surface were determined. The obtained information was useful for describing the change in catalytic performance of the synthesized catalysts.

2. Experimental

2.1. Catalyst preparation

The nanoscale zirconia (ZrO_2) was prepared by the precipitation method. It was carried out by slowly adding a solution of zirconium salt precursors such as zirconyl nitrate [$ZrO(NO_3)_2$] (0.15 M) into a well-stirred precipitating solution of ammonium hydroxide (NH_4OH) (2.5 wt%) at room temperature. The pH of the solution was carefully controlled at 10. The resulting precipitate was removed, and then washed with deionized water. The obtained sample was then dried overnight at 110 °C and calcined at 450 °C for 3 h at various temperature ramping rates such as 1.0, 2.5, 5.0, 7.5 and 10.0 °C/min. Zirconia catalysts prepared by using these temperature ramping rates were denoted as ZrO_2 (1.0), ZrO_2 (2.5), ZrO_2 (5.0), ZrO_2 (7.5) and ZrO_2 (10.0), respectively.

2.2. Catalyst characterization

2.2.1. N_2 physisorption

Measurements of BET surface area, cumulative pore volume and average pore diameter were performed by the N_2 physisorption using a Micromeritics ASAP 2020 surface area and porosity analyzer.

2.2.2. X-ray diffraction (XRD)

The XRD spectra of catalysts were measured by a SIEMENS D5000 X-ray diffractometer using Cu Kα radiation with a nickel filter over the 2θ ranging from 20° to 80°. The crystal sizes of the prepared catalysts were obtained by XRD line broadening using Scherrer's equation. The characteristic peaks at $2\theta = 28.2°$ and 31.5° for (−1 1 1) and (1 1 1) reflexes, respectively, were assigned to the monoclinic phase in ZrO_2. The characteristic peak at $2\theta = 30.2°$ for the (1 1 1) reflex in the XRD patterns represented the tetragonal phase in ZrO_2.

The percents of tetragonal and monoclinic phases in ZrO_2 were calculated by a comparison of the areas for the characteristic peaks of the monoclinic phase and the tetragonal phase. The percent of each phase was determined by means of the Gaussian areas $h \times w$, where h and w are the height and half-height width of the corresponding XRD characteristic peak as follows [4]:

$$\%\ \text{monoclinic phase} = \frac{\sum(h \times w)\ \text{monoclinic phase}}{\sum(h \times w)\ \text{monoclinic and tetragonal phase}}$$

$$\%\ \text{tetragonal phase} = \frac{\sum(h \times w)\ \text{tetragonal phase}}{\sum(h \times w)\ \text{monoclinic and tetragonal phase}}$$

2.2.3. Transmission electron microscopy (TEM)

Catalyst crystallite size and the diffraction pattern were obtained using a JEOL JEM-2010 transmission electron microscope operated at 200 kV with an optical point to point resolution of 0.23 nm at National Metal and Materials Technology Center (MTEC). The sample was dispersed in ethanol prior to the TEM measurement.

2.2.4. Temperature-programmed desorption (TPD)

Temperature-programmed desorption of ammonia and carbon dioxide (NH_3- and CO_2-TPD) was used to determine the acid-base properties of catalysts. TPD experiments were carried out using a flow apparatus. The catalyst sample (0.1 g) was treated at its calcination temperature (450 °C) in a helium flow for 1 h and then saturated with a 15% NH_3/He mixture or a pure CO_2 flow after cooling to 100 °C. After purging with the helium at 100 °C for 1 h to remove weakly physisorbed NH_3 or CO_2, the sample was heated to 450 °C at a rate of 20 °C/min in a helium flow (50 cm^3/min). The amount of acid-base sites on the catalyst surface was calculated from the desorption amount of NH_3 and CO_2, respectively. It was determined by measuring the areas of the desorption profiles obtained from a Micromeritics ChemiSorb 2750 pulse chemisorption system analyzer. For the broad desorption peak, it was separated into many sub-peaks by using the Fityk program for peak fitting. All areas of sub-peaks were summed to calculate the total amount of acid and base sites.

2.2.5. Electron spin resonance spectroscopy (ESR)

Electron spin configuration was detected by using electron spin resonance spectroscopy (ESR) (JEOL model JES-RE2X) at the Scientific and Technological Research Equipment Center (STREC), Chulalongkorn University. The sample was degassed before measurement at room temperature.

2.2.6. X-ray photoelectron spectroscopy (XPS)

The XPS spectra and the binding energy of ZrO_2 catalysts were determined using a Kratos Amicus X-ray photoelectron spectrometer. The analyses were carried out with Mg Kα X-ray source under a working pressure of 1×10^{-6} Pa at current of 20 mA and 12 kV, resolution of 0.1 eV/step, and pass energy at 75 eV. The binding energy was calibrated using the C 1s peak at 285.0 eV as reference.

2.3. Reaction study

Isosynthesis was carried out at 400 °C and atmospheric pressure in a fixed-bed quartz reactor fed with a mixture of $CO/H_2/N_2 = 10/10/5$ cm^3/min. The catalyst sample of 2 g was used in each run. The reactor effluent samples were taken at intervals of 1.5 h and analyzed using the gas chromatography technique. Thermal conductivity detectors (TCD) with molecular sieve 5A and Porapak-Q columns was used to detect the CO and CO_2, respectively. A flame ionization detector (FID) with a VZ-10 column was used to detect the light hydrocarbons such as C_1–C_4 hydrocarbons. The steady-state rate for all catalysts was obtained after 20 h.

3. Results and discussion

3.1. Physical properties

By using different temperature ramping rates during calcination, both crystal phase and crystallite size of the synthesized nanoscale ZrO_2 catalysts were changed. The XRD spectra of all ZrO_2 catalysts are illustrated in Fig. 1. It shows that ZrO_2 catalysts with various heating rates of calcination exhibit similar XRD peaks at $2\theta = 28.2°$ and 31.5° assigned to the monoclinic phase and at $2\theta = 30.2°$ assigned to the tetragonal phase. The characteristic peak areas of monoclinic and tetragonal phases (Fig. 1) indicated that the latter is more dominant than the former upon increasing temperature ramping rate during calcination. In addition, the phase composition of each ZrO_2 catalyst can be calculated as shown in Table 1. The results

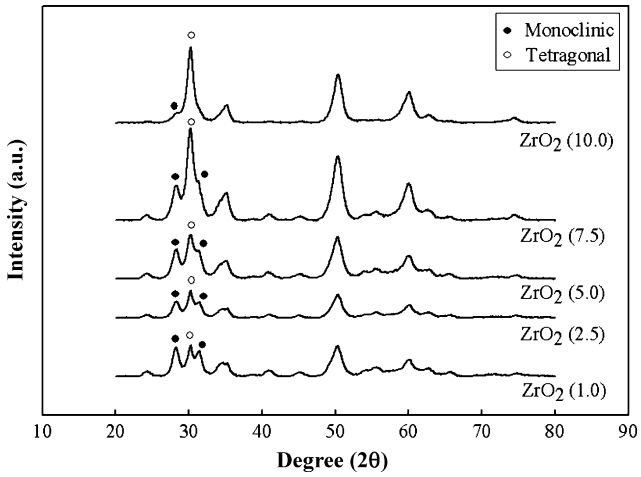

Fig. 1. XRD patterns of ZrO_2 catalysts calcined at various temperature ramping rates.

show that the fraction of the tetragonal phase increases with the increased temperature ramping rate during calcination. According to monoclinic-tetragonal phase transformation of zirconia, the tetragonal phase should be formed above 1170 °C [12], but the zirconia prepared by precipitation from aqueous salt solution can be formed as a metastable tetragonal phase at low temperature as seen in this work. Moreover, the transformation of the metastable tetragonal form into the monoclinic form was probably due to the lower surface energy of the tetragonal phase compared to monoclinic phase [13,14]. In fact, phase transformation of catalyst can take place by varying not only the calcination temperature but also the heating rate of calcination. In this case, lower temperature ramping rates would result in better heat distribution over the surface and longer contact times. Thus, this may contribute to higher stabilized crystal phase of ZrO_2, leading to more monoclinic phase present. Furthermore, the tetragonal phase that appeared was attributed to the size effect. Garvie [15] reported that the tetragonal phase appeared below a critical crystallite size about 30 nm and above that point the tetragonal could not be stabilized at room temperature. The average crystallite sizes of each phase being present

Table 1
Characteristics of ZrO_2 catalysts calcined at various temperature ramping rates

Catalysts	BET S.A.[a] (m^2/g)	Cumulative pore volume[b] (cm^3/g)	Average pore diameter[c] (nm)	Crystal size[d] (nm)		Crystal phase	Acid sites[e] (μmol/g)	Base sites[f] (μmol/g)
				M[g]	T[h]			
ZrO_2 (1.0)	92	0.169	4.9	9.8	8.3	71% M + 29% T	389	188
ZrO_2 (2.5)	100	0.172	4.7	11.4	11.3	54% M + 46% T	403	277
ZrO_2 (5.0)	103	0.199	5.4	8.7	8.6	57% M + 43% T	413	278
ZrO_2 (7.5)	106	0.191	5.0	7.5	7.5	45% M + 55% T	387	224
ZrO_2 (10.0)	100	0.139	3.7	6.5	9.0	15% M + 85% T	428	379

[a] Error of measurement ±5%.
[b] BJH desorption cumulative volume of pores between 1.7 and 300 nm diameter.
[c] BJH desorption average pore diameter.
[d] Determined by XRD line broadening using Scherrer's equation [24].
[e] Measured by NH_3-TPD.
[f] Measured by CO_2-TPD.
[g] Monoclinic phase in ZrO_2.
[h] Tetragonal phase in ZrO_2.

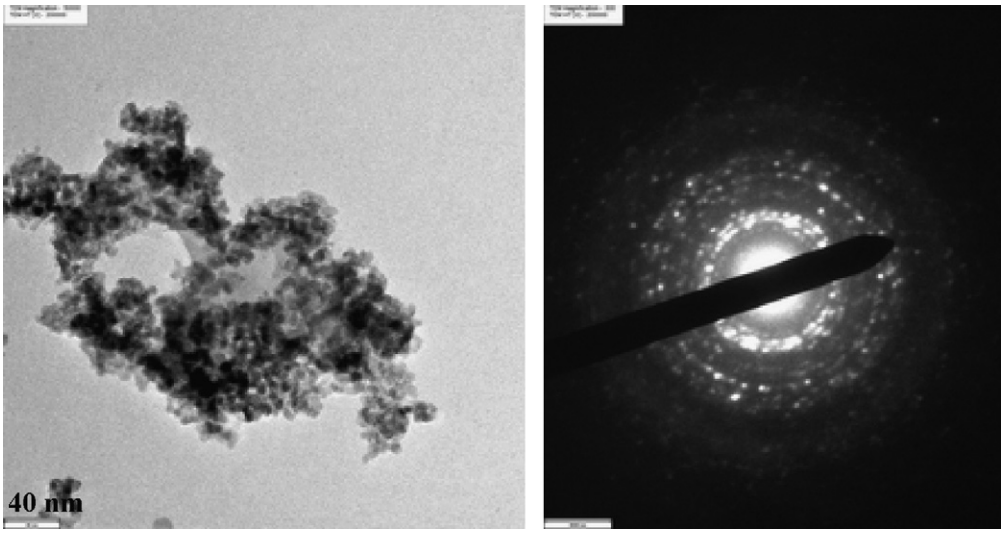

Fig. 2. TEM micrograph of ZrO_2 (1.0) catalyst and its TEM micrograph with electron diffraction mode.

in all catalysts were calculated using the XRD line broadening regarding to its characteristic peaks and also listed in Table 1, which indicates the values ranging between 7 and 12 nm. Therefore, all ZrO_2 catalysts had mixed phases of monoclinic and tetragonal phases because their crystallite sizes were less than 30 nm. Moreover, it was revealed that ZrO_2 catalysts in this work were in the nanoscale. However, for better understanding on the crystallite size, it should be determined by means of the TEM technique. Apparently, TEM can provide the image of particle characteristics in terms of the crystallite size or the particle size and geometry as well. The TEM micrographs of all catalysts are similar and the typical micrograph of the ZrO_2 (1.0) catalyst is illustrated in Fig. 2. The TEM images clearly indicated that all ZrO_2 catalysts were in nano-size. In addition, TEM with the electron diffraction mode can determine the crystallographic structure of catalyst. From the electron diffraction results (Fig. 2), it is revealed that the nanoscale ZrO_2 catalyst is polycrystallite.

The other physical properties of ZrO_2 catalysts characterized by means of N_2 physisorption such as BET surface area, cumulative pore volume and average pore diameter are also summarized in Table 1. These nanoscale ZrO_2 catalysts had specific surface areas ranging between ca. 92 and 106 m^2/g. For cumulative pore volume and average pore diameter, no significant difference was observed in all ZrO_2 catalysts, except for ZrO_2 (10.0) where the decrease in both properties was evident. This was probably due to sintering of catalysts when a high temperature ramping rate during calcination was applied. Therefore, it can be concluded that the temperature ramping rate during calcination does not significantly affect these physical properties corresponding to their crystallite sizes.

3.2. Acid-base properties

The acid-base properties of the catalysts were measured by using NH_3- and CO_2-TPD techniques, respectively. The NH_3- and CO_2-TPD profiles of ZrO_2 catalysts with various temperature ramping rates during calcination are shown in Figs. 3 and 4, respectively. The amounts of acid and base sites summarized in Table 1 were calculated from the area below the curve of TPD profile. The characteristic peaks of these profiles are assigned to their desorption temperatures indicating the strength of Lewis surface sites. From NH_3-TPD results Ma et al. [16] have reported that NH_3 desorption peaks located at ca. 200 and 300 °C for ZrO_2 catalysts are corresponding to weak acid sites and moderate acid sites, respectively. Moreover, both peaks of monoclinic ZrO_2 exhibit slightly higher amount of acid sites compared to the tetragonal ZrO_2. In this work, all NH_3-TPD profiles in Fig. 3 exhibit similar desorption profiles consisting mainly of weak acid sites. It can be observed that the amount of acid sites is in the range of ca. 387–428 μmol/g as listed in Table 1 indicates insignificant difference. The acidity of these catalysts slightly changes when the fraction of the tetragonal phase in ZrO_2 increases as illustrated in Fig. 5.

Based on CO_2 desorption peaks, the weak base sites, moderate base sites and strong base sites can be identified [16]. All

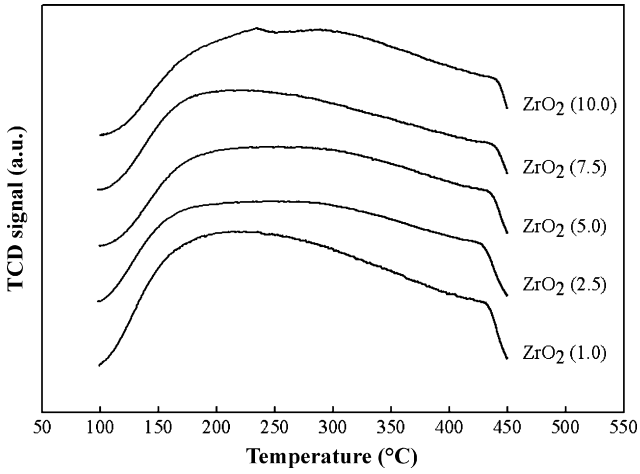

Fig. 3. NH_3-TPD profiles of catalysts.

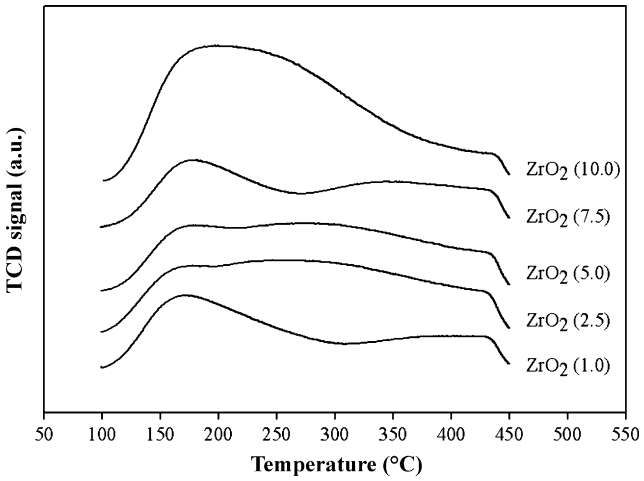

Fig. 4. CO_2-TPD profiles of catalysts.

kinds of base sites were present in the tetragonal ZrO_2 whereas only weak and moderate base sites were observed on the monoclinic ZrO_2. For CO_2-TPD profiles (Fig. 4), the CO_2 desorption peaks at low temperature appear in all profiles, suggesting that all ZrO_2 catalysts have weak base sites. However, the increase in temperature ramping rate during calcination results in higher desorption temperature and areas under its curve as well. The basicity of these catalysts increases with increase in the fraction of the tetragonal phase in ZrO_2 as shown in Fig. 5. As a result of previous work [10], the presence of more tetragonal in ZrO_2 is attributed to higher basicity of catalysts, especially for moderate and strong base sites. Therefore, the highest basicity of ZrO_2 (10.0) is due to the highest tetragonal phase in ZrO_2.

In this work, all ZrO_2 catalysts have similar physical properties such as BET surface area. Thus, acid-base properties of these catalysts are independent of the physical properties, but it can be varied with the composition of phases in ZrO_2 resulting from various heating rates during calcination.

3.3. The existence of Zr^{3+} on the surface of ZrO_2

XPS measurement is performed to identify valence electron or oxidation state of ion on the surface of catalysts. In this work, zirconium ion on the surface of ZrO_2 was investigated. A survey scan is performed before the elemental scan which was carried out for C 1s, O 1s, and Zr 3d. The binding energy of each element was referenced by the C 1s peak position at 285.0 eV. A high-resolution scan of Zr of ZrO_2 (1.0) sample showed the double peaks of Zr 3d consisting of Zr $3d_{5/2}$ and Zr $3d_{3/2}$ peaks (Fig. 6). The other ZrO_2 samples (not shown) exhibited similar results as seen in Fig. 6. It was found that there were four sub-peaks for the Zr 3d peak after deconvolution by fitting with Gaussian–Lorentzian shapes using a VISION 2 software equipped with XPS. The two major peaks at position of 182.3 and 184.8 eV were assigned to Zr $3d_{5/2}$ and Zr $3d_{3/2}$ peaks of Zr^{4+}, respectively, as reported early [17–19]. The binding energies for two small (minor) peaks shifted towards lower binding energies compared with the major peaks. The peak position of Zr^0 [19] is at 178.5 eV. Therefore, those small peaks can be attributed to peaks of zirconium ion between 0 and 4 because the positions of those peaks are in the range of peak position of Zr^0 and Zr^{4+}. However, those small peaks were shifted by 0.2–0.5 eV, which was only a little decrease in binding energies that might cause a little change in valence electron of zirconium. Therefore, those small peaks can be presumably assigned to the Zr^{3+} peak. In fact, Zr^{4+} is zirconium-based ion on the surface of synthesized ZrO_2. However, Zr^{3+} should have more chances to be detected among other zirconium ions, such as Zr^{2+}, Zr^+ and Zr^0.

Therefore, XPS measurements of ZrO_2 samples showed the existence of Zr^{3+} on their surface. However, the ESR technique is a promising method for quantifying the relative concentration of Zr^{3+} on the ZrO_2 surface, as reported in several papers [20–22] because it can certainly identify the peak position of only unpaired valence electron of ZrO_2 especially that of Zr^{3+}. For paired electron of ZrO_2 such as Zr^{4+}, it cannot be detected by means of ESR. Therefore, the ESR technique was used to com-

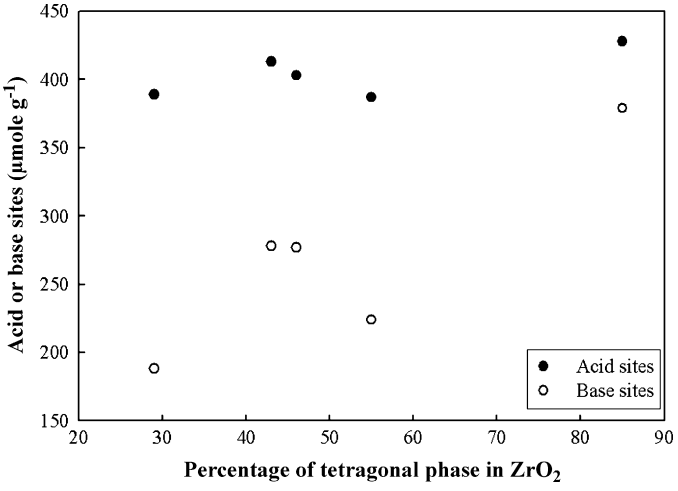

Fig. 5. Relationship between amount of acid sites and base sites and percent of tetragonal phase in ZrO_2.

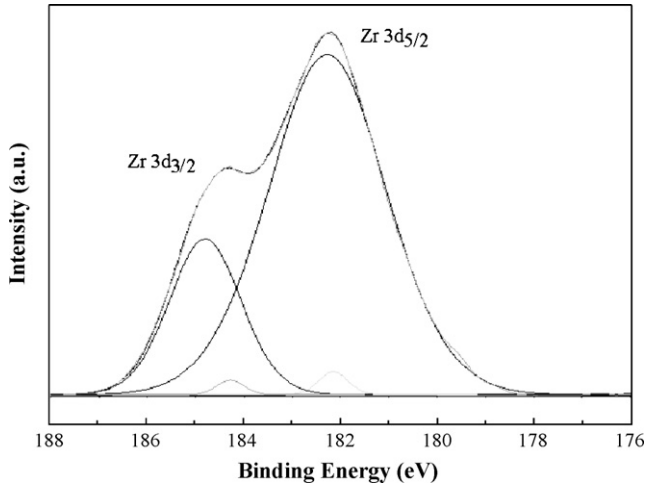

Fig. 6. XPS spectrum of Zr 3d of ZrO_2 (1.0).

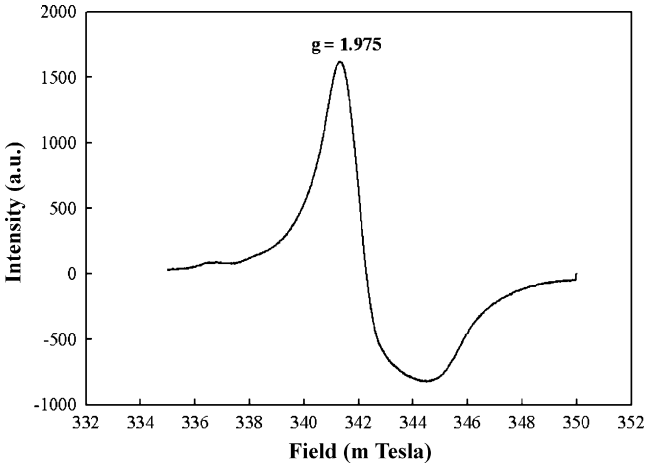

Fig. 7. ESR spectrum of ZrO_2 (1.0) catalyst.

pare the quantity of Zr^{3+} in ZrO_2 as described in the following section.

3.4. Intensity of Zr^{3+} in ZrO_2

A spin of unpaired electron was detected by means of ESR to identify defect center of zirconia, assuming the existence of Zr^{3+} sites. The Zr^{3+} signals present at $g_{\perp}\sim1.975$ and $g_{||}\sim1.957$ were very close to the positions of Zr^{3+} on the ZrO_2 surface observed by many researchers [20–22]. Only $g_{\perp}$ was considered in this work due to the apparent signal. The ESR spectra for all ZrO_2 catalysts are similar and the typical ESR spectrum of the ZrO_2 (1.0) catalyst is shown in Fig. 7, but the intensity of Zr^{3+} for all of them is significantly different. The peak height of the Zr^{3+} signal ($g_{\perp}\sim1.975$) is attributed to the quantity of Zr^{3+}. For comparison of the Zr^{3+} intensity, the weight of each ZrO_2 catalyst tested with ESR must be equal. The relative ESR intensity for various ZrO_2 catalysts is shown in Fig. 8. It is found that quantity of Zr^{3+} is different for the catalysts with various temperatures ramping rate during calcination. The result shows that Zr^{3+} gradually increases with the increase in the heating rate of calcination up to the highest intensity at ca. 5 °C/min, and then rapidly decreases beyond that value. Early researches [22,23] suggested that the Zr^{3+} center to ESR can be described as the oxygen coordinatively unsaturated zirconium sites on the ZrO_2 surface. In addition, they proposed that the removal of the surface hydroxyl accounted for the formation of the new Zr^{3+} sites. It is possibly due to the presence of hydroxyl groups combined in a position of coordinatively unsaturated sites resulting in less Zr^{3+} intensity. Therefore, the changes of Zr^{3+} intensity in this case may be attributed to loss of the surface O atoms, especially hydroxyl groups, on the ZrO_2 surface. Low heating rates during calcination can remove the hydroxyl group more than the high heating rate because the former had long times for releasing hydroxyl group compared to the latter. As seen at calcination temperature ramping rates of 7.5 and 10 °C/min, the relative intensity of Zr^{3+} obviously decreased. This is possibly due to the effect of fast increase in temperature influencing more than the effect of longer contact times. More hydroxyl groups were removed from the surface of ZrO_2 catalyst. Moreover, Fig. 9 shows the relationship between the tetragonal phase in ZrO_2 and Zr^{3+} intensity. The intensity of Zr^{3+} has the highest value at ca. 43% of the tetragonal phase in ZrO_2, then decreases almost linearly upon increasing the tetragonal phase in ZrO_2.

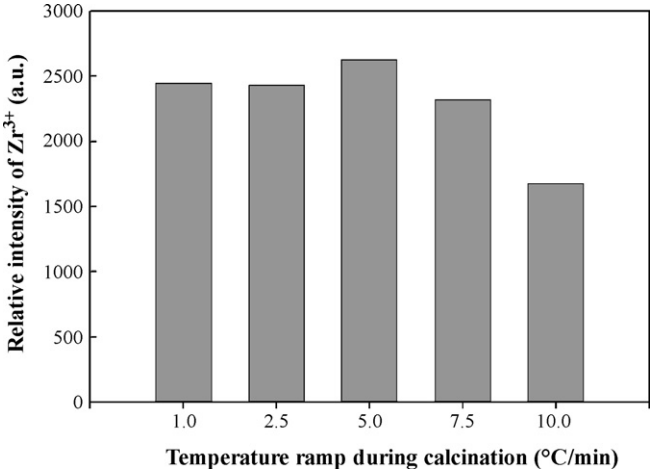

Fig. 8. Relative ESR intensity of various ZrO_2 catalysts.

3.5. Catalytic performance

The ZrO_2 catalysts with various temperature ramping rates during calcination were tested for their isosynthesis activity and selectivity at 400 °C, atmospheric pressure and CO/H_2 of 1. The steady-state rate was reached after 20 h. The results of the catalytic activities calculated from the product formations are summarized in Table 2. The amount of Zr^{3+} is a major factor affecting the product selectivity to isobutene, as shown in Fig. 10. It is obvious that the ZrO_2 (5.0) exhibited the highest concentration of Zr^{3+}, corresponding to the highest selectivity to isobutene in hydrocarbons. Considering the results obtained with temperature ramping rates during calcination of 1.0, 2.5 and 5.0 °C/min, it can be concluded that the relative intensity of Zr^{3+} is related to the heating rate of calcination. Although ZrO_2

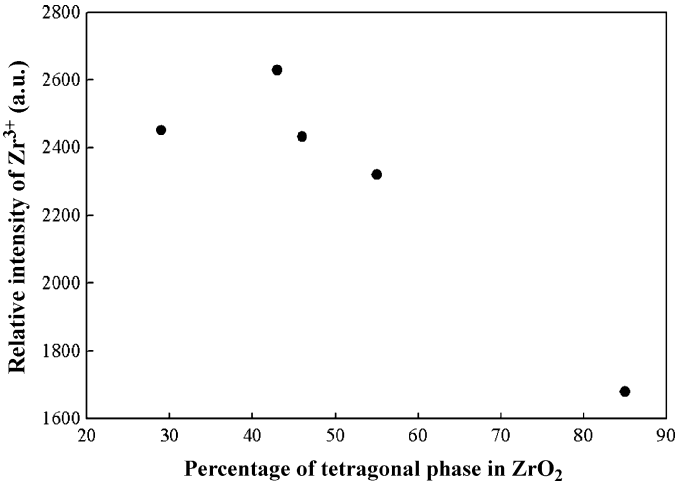

Fig. 9. Relationship between quantity of Zr^{3+} and percent of tetragonal phase in ZrO_2.

Table 2
The catalytic performance of ZrO_2 catalysts calcined at various temperature ramping rates during calcination in the isosynthesis

Catalysts	CO conversion (%)	Reaction rate[a] (μmol kg cat^{-1} s^{-1})	Product selectivity in hydrocarbons[b] (mol%)				Product selectivity (mol%)	
			C_1	C_2	C_3	i-C_4H_8	HC[c]	CO_2
ZrO_2 (1.0)	2.90	97.3	6.0	5.6 (60.4)	11.1 (87.9)	77.3	53.6	46.4
ZrO_2 (2.5)	3.97	133.0	7.6	9.0 (62.8)	14.2 (85.5)	69.2	47.4	52.6
ZrO_2 (5.0)	1.91	63.9	3.8	3.8 (65.1)	9.5 (93.5)	82.9	67.6	32.4
ZrO_2 (7.5)	1.82	61.0	3.8	3.7 (66.9)	9.5 (94.0)	82.9	68.4	31.6
ZrO_2 (10.0)	3.15	105.5	7.7	7.3 (60.2)	11.5 (86.1)	73.4	52.6	47.4

Reaction conditions were at 400 °C, 1 atm and $CO/H_2 = 1$.
[a] Steady-state of reaction was reached at 20 h.
[b] Parentheses are percent of olefins present in products.
[c] Total hydrocarbons.

(5.0) and ZrO_2 (7.5) resulted in the highest product selectivity to isobutene, the two catalysts have different Zr^{3+} intensities. ZrO_2 (7.5) have lower quantity of Zr^{3+} than ZrO_2 (5.0). Thus, both catalysts would have another factor affecting the selectivity to isobutene in hydrocarbons, which may be attributed to the presence of the tetragonal phase in ZrO_2. Increase in the tetragonal phase in ZrO_2 probably results in higher selectivity to isobutene in hydrocarbons. Therefore, the increase in the tetragonal phase in ZrO_2 (7.5) leads to the high selectivity to isobutene in hydrocarbons even at a lower content of Zr^{3+}. No direct relationship between the quantity of Zr^{3+} or the fraction of the tetragonal phase in ZrO_2 and isobutene selectivity was found. It can be mentioned that the effects of amounts of Zr^{3+} and the tetragonal phase present in ZrO_2 can be superimposed on each other. Thus, the observed selectivities to isobutene were roughly equal. By comparison of the ZrO_2 (7.5) and ZrO_2 (10.0) performance, it can be proposed that the effect of Zr^{3+} intensity is more pronounced than that of the tetragonal phase. As a result, the latter exhibits lower selectivity to isobutene in hydrocarbons. The presence of the tetragonal phase in ZrO_2 is apparently related to the amount of acid and base sites as reported by Khaodee et al. [10]. Therefore, there were many factors affecting the product selectivity to isobutene. However, the intensity of Zr^{3+} and the tetragonal phase in ZrO_2 were dominant factors. Based on the results of Li et al. [11], there was a close linear relation between

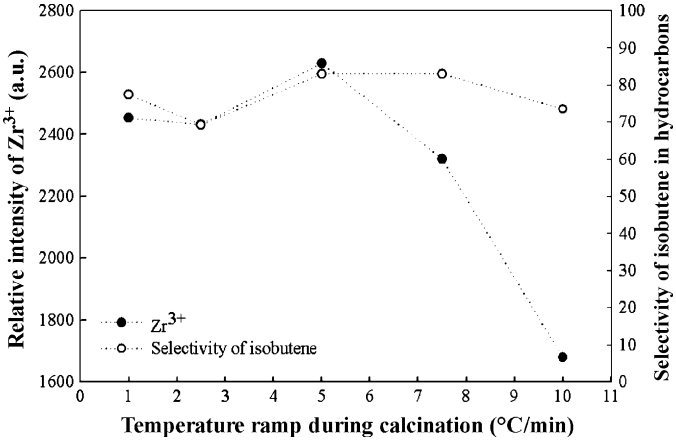

Fig. 10. Relationship between intensity of Zr^{3+} along with selectivity of isobutene in hydrocarbons and temperature ramping rates during calcination.

Zr^{3+} ion and the selectivity to isobutene for the reaction over ZrO_2. Those results showed that Zr^{3+} ion might be involved in CO hydrogenation, possibly suggesting the mechanism of the catalytic reaction via a surface species Zr(III)$(CO)_2$.

It can be concluded that selectivity to isobutene in hydrocarbons is dependent on the intensity of Zr^{3+} upon the temperature ramping rate during calcination less than 5.0 °C/min. For heating rates of calcination more than 5.0 °C/min, the product selectivity to isobutene depends on not only the quantity of Zr^{3+} but also on the tetragonal phase in ZrO_2. The direct relationship between Zr^{3+} intensity or fraction of the tetragonal phase in ZrO_2 and the selectivity to isobutene in hydrocarbons might not be observed for these catalysts. Therefore, the key factor affecting the product selectivity consists of intensity of Zr^{3+} and the tetragonal phase composition in ZrO_2. In addition, the tetragonal phase in ZrO_2 was dependent on the basicity of catalysts. Thus, base properties results in the product selectivity to isobutene as seen in the previous works [4,7–9].

In addition, the selectivity to total hydrocarbons as reported in Table 2 show similar trend to that for the selectivity to isobutene in hydrocarbons. The amount of acid sites is not directly related to the activity. The tendency of the activity of ZrO_2 catalysts is opposite to that of the product selectivity to isobutene; for instance, activity decreases with increasing selectivity to isobutene in hydrocarbons. Table 2 shows that ZrO_2 (2.5) exhibits the highest activity among all ZrO_2 catalysts.

4. Conclusions

The effect of temperature ramping rates during calcination on the characteristics and catalytic performance for isosynthesis of nanoscale zirconia catalysts was investigated. The mixed phase of tetragonal and monoclinic phases of zirconia catalysts (29–85% T) could be achieved when the heating rate of calcination was varied in the range of 1.0–10.0 °C/min. The tetragonal phase composition increased with increasing temperature ramping rate during calcination. For the other physical properties such as BET surface area, cumulative pore volume and pore diameter, there was insignificant effect found based on the change in the temperature ramping rate. For the surface properties of zirconia catalysts, the intensity of Zr^{3+} changed with the varying heating rate of calcination. The results showed that ZrO_2 (5.0) had the

highest product selectivity to isobutene in hydrocarbons due to the maximum quantity of Zr^{3+} present in the sample. However, both of the tetragonal phase in zirconia and intensity of Zr^{3+} influenced the selectivity to isobutene. ZrO_2 (2.5) showed the highest activity among all zirconia catalysts.

Acknowledgements

The support from the National Research Council of Thailand (NRCT) is greatly appreciated. The authors would like to thank Assistant Professor Joongjai Panpranot and Assistant Professor Okorn Mekasuwandamrong for useful discussion.

References

[1] I. Wender, Fuel Proc. Tech. 48 (1996) 189.
[2] H. Pichler, K.H. Ziesecke, Brennst. Chem. 30 (1949) 13.
[3] H. Pichler, K.H. Ziesecke, B. Traeger, Brennst. Chem. 30 (1949) 333.
[4] C. Su, J. Li, D. He, Z. Cheng, Q. Zhu, Appl. Catal. A: General 202 (2000) 81.
[5] C. Su, D. He, J. Li, Z. Chen, Q. Zhu, J. Mol. Catal. A: Chem. 153 (2000) 139.
[6] K. Maruya, T. Komiya, T. Hayakawa, L. Lu, M. Yashima, J. Mol. Catal. A: Chem. 159 (2000) 97.
[7] Y. Li, D. He, Z. Cheng, C. Su, J. Li, Q. Zhu, J. Mol. Catal. A: Chem. 175 (2001) 267.
[8] Y. Li, D. He, Y. Yuan, Z. Cheng, Q. Zhu, Fuel 81 (2002) 1611.
[9] Y. Li, D. He, Q. Zhu, X. Zhang, B. Xu, J. Catal. 221 (2004) 584.
[10] W. Khaodee, B. Jongsomjit, S. Assabumrungrat, P. Praserthdam, S. Goto, Catal. Commun. 8 (2007) 548.
[11] W. Li, Y. Yin, L. Feng, P. Zheng, Acta Physico—Chimica Sinica 12 (1996) 1074.
[12] P.D.L. Mercera, J.G. van Ommen, E.B.M. Doesburg, A.J. Burggraaf, J.R.H. Ross, Appl. Catal. 71 (1991) 363.
[13] E. Tani, M. Yoshimura, S. Somiya, J. Am. Ceram. Soc. 66 (1982) 11.
[14] M.I. Osendi, J.S. Moya, C.J. Sena, J. Soria, J. Am. Ceram. Soc. 68 (1985) 135.
[15] R.C. Garvie, J. Phys. Chem. 82 (1978) 218.
[16] Z.-Y. Ma, C. Yang, W. Wei, W.-H. Li, Y.-H. Sun, J. Mol. Catal. A: Chem. 227 (2005) 119.
[17] S. Ardizzone, C.L. Bianchi, M. Signoretto, Appl. Surf. Sci. 136 (1998) 213.
[18] S. Tsunekawa, K. Asami, S. Ito, M. Yashima, T. Sugimoto, Appl. Surf. Sci. 252 (2005) 1651.
[19] C.D. Wagner, W.M. Riggs, L.E. Davis, Handbook of X-ray Photoelectron Spectroscopy, Eden Prairie, Minesoda, 1979, p. 55344.
[20] C. Moterra, E. Giamello, L. Orio, M. Volante, J. Phys. Chem. 94 (1990) 3111.
[21] H. Liu, X. Zhang, Q. Xue, J. Phys. Chem. 99 (1995) 332.
[22] Q. Zhao, X. Wang, T. Cai, Appl. Surf. Sci. 225 (2004) 7.
[23] M. Anpo, T. Nomura, Res. Chem. Intermed. 13 (1990) 195.
[24] H.P. Klug, L.E. Alexander, X-ray Diffraction Procedures for Polycrystalline Amorphous Materials, Wiley, New York, 1974.